



Picoliter Enzyme Reactor on Nanofluidic Device Exceeding Bulk Reaction Rate

Journal:	<i>Analyst</i>
Manuscript ID	AN-ART-05-2020-000998.R1
Article Type:	Paper
Date Submitted by the Author:	29-Jun-2020
Complete List of Authors:	Yamamoto, Koki; The University of Tokyo Morikawa, Kyojiro; The University of Tokyo, Department of Applied Chemistry, School of Engineering Imanaka, Hiroyuki; Okayama University, Division of Chemistry and Biochemistry, Graduate School of Natural Science and Technology Imamura, Koreyoshi; Okayama University, Division of Chemistry and Biochemistry, Graduate School of Natural Science and Technology Kitamori, Takehiko; The University of Tokyo

Picoliter Enzyme Reactor on Nanofluidic Device Exceeding Bulk Reaction Rate

Koki Yamamoto¹, Kyojiro Morikawa^{2,*}, Hiroyuki Imanaka³, Koreyoshi Imamura³, and Takehiko Kitamori^{1,2,*}

1 Department of Bioengineering, School of Engineering, The University of Tokyo, 7-3-1 Hongo, Bunkyo, Tokyo 113-8656, Japan

2 Department of Applied Chemistry, School of Engineering, The University of Tokyo, 7-3-1 Hongo, Bunkyo, Tokyo 113-8656, Japan

3 Division of Chemistry and Biochemistry, Graduate School of Natural Science and Technology, Okayama University, 3-1-1 Tsushima-Naka, Kita-Ku, Okayama 700-8530, Japan.

Corresponding authors

* To whom correspondence should be addressed:

Kyojiro Morikawa: morikawa@icl.t.u-tokyo.ac.jp

Takehiko Kitamori: kitamori@icl.t.u-tokyo.ac.jp

Abstract

Single-cell analyses have recently become important to understand cell heterogeneity, the mechanism of cell function, and diseases. In contrast to single-cell analyses that target nucleic acids, single-cell protein analyses still pose challenges. We have proposed a general concept of integration and extended this concept to the 10–1000 nm scale with femtoliter-picoliter volume which are smaller than the volume of a single cell exploring ultimate analytical performances (e.g. single-cell target proteomics). However, single-cell shotgun proteomics, which are used to analyze even unknown proteins, is still challenging because there is no digestion column with picoliter volume. The issues were long reaction time (overnight) and much larger reaction volume (microliter) in the conventional bulk method. In this study, an ultra-fast picoliter enzyme reactor using nanochannel was developed. A device which channel depth was 300 nm and volume was 32.4 pL was fabricated. To prevent self-digestion of trypsin (enzyme), the picoliter enzyme reactor was prepared by immobilizing trypsinogen which was activated to trypsin by enterokinase. The enzyme density by trypsinogen immobilization process was 2.5 times higher than that by conventional trypsin immobilization process. Furthermore, apparent enzyme concentration was 36 times higher due to extremely high surface-to-volume ratio of the nanochannel, compared to limit concentration in the bulk. Finally, the enzyme reaction in the picoliter enzyme reactor was accelerated 25 times compared to that in the bulk. Using the picoliter enzyme reactor, protein solution with picoliter volume will be digested without self-digestion and artificial modification, which will greatly contribute to single-cell shotgun proteomics.

Introduction

Single-cell analyses have recently become important to understand cell heterogeneity, the mechanism of cell function, and diseases.¹⁻⁵ In contrast to single-cell analyses that target nucleic acids,⁶ single-cell protein analyses still pose challenges due to differences in the analyte properties. Nucleic acids are composed of only 4 bases, and they can be amplified by polymerase chain reaction (PCR), and easily separated using techniques such as capillary electrophoresis or hybridization. On the other hand, proteins are composed of 20 and more different amino acids, which have a three-dimensional molecular structure, and they cannot be amplified. As a result, various separation and detection techniques are required, such as western blotting, enzyme-linked immunosorbent assay (ELISA), liquid chromatography (LC), or electrophoresis for separation, and absorbance and fluorescence spectroscopies, or mass spectrometry (MS) for detection. In addition, considering the picoliter (pL; 10^{-12} L) volume of a single cell and the very small number and wide dynamic range of analyte protein molecules in the cell, ultimate analytical performance is required in pretreatment, separation, and detection.^{7,8} It is still difficult to use the bulk method because the volume of the analytical field is much larger than pL order. In the bulk method, analyte molecules are significantly diluted often down to the detection limit. Therefore, entire chemical processing for single-cell analysis should be integrated into spaces smaller than single cells to prevent analyte dilution.

1
2
3
4
5
6
7
8
9
10
11
12
13
14
15
16
17
18
19
20
21
22
23
24
25
26
27
28
29
30
31
32
33
34
35
36
37
38
39
40
41
42
43
44
45
46
47
48
49
50
51
52
53
54
55
56
57
58
59
60

Microfluidics using 10-100 μm channels has been developed in the last two decades.^{9,10}

Our group has established a general method for the integration of chemical processing to realize miniaturized analytical devices.¹¹ The methodology is micro unit operation (MUO) and continuous flow chemical processing (CFCP). In this methodology, bulk-scale chemical operations are replaced by MUOs, and the different MUOs are connected to each other in parallel and serially, similar to an electrical circuit. Considering that the volumes of the microspaces are comparable to the volume of a single cell, many types of MUOs have been developed for the chemical processing of cells.¹²⁻¹⁴ More recently, our group pioneered nanofluidics using 10-1000 nm channels with controlled dimensions, and developed basic technologies for fabrication, fluid control, and detection.^{15,16} The volume of the nanochannel is on the scale of femtoliters (fL; 10^{-15} L), which is much smaller than that of a single cell. The smallness of such a space means a fL pipette and a pL flask can be used to handle fL-pL liquids.¹⁷ The chemical processing of even countable protein molecules has been developed (single-molecule ELISA) by exploiting the high surface-to-volume ratio of the nanofluidic spaces.¹⁸ The combination of MUOs and nano unit operations (NUOs) has finally realized the protein analysis of cellular release of a living single cell with integration of a fL pipette, a pL flask, and single-molecule ELISA.¹⁹

However, single-cell shotgun proteomics, which are used to analyze even unknown proteins, is still challenging. In shotgun proteomics, proteins are digested into peptide fragments

1
2
3
4
5
6 by hydrolysis (typically trypsin) and analyzed using liquid chromatography-mass spectrometry
7
8
9 (LC-MS). To develop single-cell shotgun proteomics, the development of NUOs such as for
10
11
12 protein digestion and LC-MS are required. Femtoliter chromatography using nanochannels has
13
14
15 been developed for LC, and ultra-high performance of 14,000 plate numbers (one order higher
16
17
18 than conventional high-performance liquid chromatography (HPLC)) were reported.²⁰ For MS
19
20
21 detection, a pL droplet shooter has been under development for interface with MS.²¹ Therefore,
22
23
24 NUOs for LC-MS that can analyze fL-pL samples have also been under development. However,
25
26
27 there is no NUO for protein digestion, because there are still two main issues to address: reaction
28
29
30 time and reaction volume. For protein digestion in the bulk, trypsin is typically used²², although
31
32
33 it is known to induce self-digestion.²³⁻²⁶ To prevent excessive contamination by self-digestion
34
35
36 fragments and trypsin itself,²⁷ low trypsin concentrations (typically, trypsin:sample protein =
37
38
39 1:100) are generally used and the limitation is approximately 0.5 μM .²⁸ To compensate for the
40
41
42 limited concentration of trypsin, long incubation times (overnight) are required. However, such
43
44
45 long incubation times sometimes induce artificial modification,²⁹⁻³² which affects the peptide
46
47
48 structure and properties. Therefore, it is essential to develop a digestion method to achieve high-
49
50
51 efficiency, ultra-fast protein digestion for shotgun proteomics. For smaller reaction volumes,
52
53
54 many groups have developed reactors that use microspaces and packed beads or monolithic
55
56
57 columns modified with trypsin on the surface, which are called microreactors/nanoreactors.³³⁻³⁶
58
59
60

1
2
3
4
5
6
7 However, the volumes of these microreactors are still only microliter-nanoliter (μL - nL). As a
8
9 result, it is still difficult to apply protein digestion in single-cell analysis.
10

11
12 To overcome the limitation of reaction in the bulk and in a microreactor, we conceived
13
14 a reactor with reactant-immobilized nanochannels. In this reactor, apparent concentration of
15
16 reactant can overcome the limit concentration in the bulk due to extremely high surface-to-volume
17
18 ratio in the nanochannels. In this study, the idea of the nanofluidic reactor was applied to picoliter
19
20 enzyme reactor for protein digestion in single-cell analysis. Trypsin is immobilized on the size-
21
22 regulated nanochannel surfaces with high density in a newly invented method as described below,
23
24 and the liquid volume in the reaction field is only on the scale of pL . As a result, the apparent
25
26 trypsin concentration, which is determined by (number of trypsin molecules on the
27
28 surface)/(volume of reaction field), will be significantly increased by the high surface-to-volume
29
30 ratio in the nanochannel. In this study, we designed a reactor with an apparent trypsin
31
32 concentration that exceeds the concentration limit in the bulk, and verified whether a high
33
34 concentration and fast enzyme reaction were achieved.
35
36
37
38
39
40
41
42
43
44
45
46
47
48
49
50

51 **Design**

52
53 To develop a reactor that can be applied for single-cell analysis devices, a pL volume of
54
55 the reaction field is required, which is the same order as a single-cell volume. Precursor form of
56
57
58
59
60

1
2
3
4
5
6 protease, trypsinogen, were immobilized on the nanochannel surface of the reactor to prevent self-
7
8
9 digestion in the immobilization step. The apparent enzyme concentration $[E]_{app}$, is calculated by
10
11
12 (number of trypsin molecules on the surface)/(volume of reaction field) according to the following
13
14
15 equation:

$$[E]_{app} = \frac{LW\rho}{LWd} = \frac{\rho}{d} \quad (1)$$

16
17
18
19
20
21
22
23
24 where L represents the length of the reaction field, W represents the width of the reaction field, d
25
26
27 represents the depth of the reaction field, and ρ represents the enzyme density. Therefore, a high
28
29
30 $[E]_{app}$ is achieved by setting a nanometer scale d as shown in Figure 1. The size of the nanochannel
31
32
33 and reaction field is shown in Figure 2. The width of the nanochannel was 18 μm , the depth was
34
35
36 300 nm, and the total length was 8.0 mm. The trypsin precursor molecules were immobilized on
37
38
39 the bottom surface of the nanochannel within a 6.0 mm long region. In this design, the volume of
40
41
42 reaction field was 32 pL, and the apparent enzyme concentration was calculated to $10^1 \mu\text{M}$ when
43
44
45 the enzyme density was $10^3 \text{ molecules}/\mu\text{m}^2$, which exceeded the bulk limit concentration of
46
47
48 approximately 0.5 μM by one order.
49
50
51
52
53

54 **Experimental**

55
56
57 Chemicals and Materials:
58
59
60

1
2
3
4
5
6 (3-Aminopropyl) triethoxysilane (APTES) was purchased from Tokyo Chemical
7
8
9 Industry (Tokyo, Japan). Trimethoxysilane-poly(ethyleneglycol) (TMS-PEG; MW = 5 kDa) was
10
11
12 purchased from NANOCS (New York, NY, USA). Glutaraldehyde (25%) was purchased from
13
14
15 Wako Pure Chemical Industries (Osaka, Japan). Trypsin from bovine pancreas ((TPCK-treated,
16
17
18 10 000 BAEE units/mg protein), EC 3.4. 21.4, MW = 23.8 kDa), trypsinogen from bovine
19
20
21 pancreas (EC 3.4. 23, MW = 24.0 kDa) and *N* α -benzoyl-DL-arginine *p*-nitroaniline (BAPNA)
22
23
24 were purchased from Sigma-Aldrich (St. Louis, MO, USA). Recombinant enterokinase (EC
25
26
27 3.4.21.9 MW = 26.3 kDa) was purchased from Merck KGaA (Darmstadt, Germany). Anti-trypsin
28
29
30 antibody (ab17263) was purchased from Abcam (Tokyo, Japan). Labeling of anti-trypsin with a
31
32
33 fluorescent dye (Alexa 488) was conducted using an Alexa Fluor™ 488 Antibody labeling kit
34
35
36 (Thermo Fisher Scientific, Waltham, MA, USA). All solutions were filtered with a 0.22 μ m
37
38
39 syringe filter to prevent clogging of the channel.
40
41
42
43
44

45 Device fabrication:

46
47
48 Nanochannels were fabricated on a fused-silica glass substrate (70 \times 30 mm, VIOSIL-
49
50
51 SQ, Shin-Etsu Chemical Co., Ltd., Japan) using electron-beam lithography and dry etching.
52
53
54 Microchannels (width: 500 μ m, depth: 10 μ m, length: 60 mm) with an inlet hole and detection
55
56
57 chambers (diameter: 15 μ m, depth: 10 μ m) were fabricated on another glass substrate by
58
59
60

1
2
3
4
5
6 photolithography and dry etching. The detailed fabrication process has been described in our
7
8
9 previous reports.³⁷⁻³⁹ APTES was partially modified for the reaction field on the microchannel
10
11
12 substrate by vacuum ultraviolet light.⁴⁰ The two substrates were bonded using a low-temperature
13
14
15 bonding method at 110 °C for 2 h.⁴⁰⁻⁴²
16
17
18
19
20

21 Protease immobilization:

22
23
24 To reduce the potential for nonspecific protein adsorption onto the nanochannel surfaces,
25
26
27 the surfaces were chemically modified with 0.1 wt% PEG in water/ethanol solution. For chemical
28
29
30 crosslinking between APTES and protease via protein amino group, 2.5% glutaraldehyde solution
31
32
33 in 100 mM borate buffer (pH 8.0) was contacted with the APTES coated surface to graft the
34
35
36 aldehyde groups. Trypsinogen was coupled to the support by pumping 2.0 mg/mL trypsinogen in
37
38
39 a 100 mM borate buffer containing 20 mM CaCl₂ through the nanochannel at 4 °C for 2 h. Finally,
40
41
42 trypsinogen was converted into the active form trypsin by 0.01 unit enterokinase in 20 mM Tris-
43
44
45 HCl (pH 7.4) containing 2 mM CaCl₂ and 50 mM NaCl at 23 °C for 2 h. All solutions were
46
47
48 introduced to the nanochannels using a pressure controller. This process is an original new
49
50
51 immobilization method we have termed the trypsinogen immobilization process. For comparison
52
53
54 with the immobilization method, a nanochannel in another device was modified with APTES,
55
56
57 PEG, and glutaraldehyde using the same conditions as the trypsinogen immobilization process,
58
59
60

1
2
3
4
5
6 and 2.0 mg/mL trypsin in a 100 mM borate buffer containing 20 mM CaCl₂ was passed through
7
8
9 the nanochannel at 4 °C for 2 h. This trypsin immobilization method is a typical method to
10
11
12 immobilize trypsin on a surface.^{43,44}
13
14
15
16
17

18 Measurement of immobilization density of trypsin:

19

20
21 To measure the immobilized trypsin density, 100 nM Alexa488-labeled anti-trypsin
22
23 (Monoclonal antibody) in PBS (pH 7.4) was introduced, and the increase of intensity in the
24
25 immobilized trypsin region was observed using fluorescence microscopy. Anti-trypsin molecules
26
27 were combined with trypsin molecules by immunochemical reaction and were then detected by
28
29 fluorescence microscopy. A fluorescence microscope (IX73P2F, Olympus, Japan) equipped with
30
31 a charge-coupled device (CCD) camera (C9100-13, Hamamatsu Photonics K.K., Japan) was used
32
33 to acquire fluorescence micrographs of the immobilized trypsin region. Fluorescence signals
34
35 resulting from excitation induced using a mercury lamp were collected using a 20× objective lens
36
37 with a numerical aperture (NA) of 0.46. From micrographs obtained using Aquacosmos software
38
39 (Hamamatsu Photonics K.K., Japan), the immobilized trypsin density was calculated from the
40
41 calibrated fluorescence intensity.⁴⁰
42
43
44
45
46
47
48
49
50
51
52
53
54
55
56

57 Measurement of tryptic hydrolysis reaction:

58
59
60

1
2
3
4
5
6
7
8
9
10
11
12
13
14
15
16
17
18
19
20
21
22
23
24
25
26
27
28
29
30
31
32
33
34
35
36
37
38
39
40
41
42
43
44
45
46
47
48
49
50
51
52
53
54
55
56
57
58
59
60

Tryptic hydrolysis rate was determined with the chromogenic trypsin substrate *N*α-benzoyl-DL-arginine *p*-nitroaniline (BAPNA), which liberates the yellow colored *p*-nitroaniline upon hydrolysis. Namely, 128 μM BAPNA in 50 mM borate buffer (pH 8.0) containing 20 mM CaCl₂ was introduced through the reactor at 25 °C as shown in Figure 2. The product was monitored by the subsequent increase in absorbance at 405 nm by the photothermal optical phase shift (POPS; excitation: 405 nm, probe: 532 nm).⁴⁵ The excitation coefficient of *p*-nitroaniline at 405 nm is 9920 cm⁻¹ M⁻¹.⁴⁶ Both beams were focused on a nanochannel through an objective lens (magnification: 40×; NA: 0.75) attached to a microscope (ECLIPSE 80i, Nikon Co., Japan). After each measurement was finished, the reactor was washed with 100 mM borate buffer containing 20 mM CaCl₂ to repeat measurements in the same device. The enzyme reaction time was calculated from the measured flow velocity of BAPNA when pressure was applied from 23 kPa to 500 kPa. All operations were continuously performed by repeating the regeneration in the same device. For comparison of the reaction rate, the tryptic hydrolysis reaction in the bulk was also performed. Trypsin (final concentration 0.01 mg/mL) was added to 96-well (350 μL) plates. The hydrolysis reaction rate was measured with a microplate reader (SH-9000Lab, Corona Electric Co. Ltd., Japan) at 5 min intervals.

Results and discussion

1
2
3
4
5
6
7
8
9
10
11
12
13
14
15
16
17
18
19
20
21
22
23
24
25
26
27
28
29
30
31
32
33
34
35
36
37
38
39
40
41
42
43
44
45
46
47
48
49
50
51
52
53
54
55
56
57
58
59
60

Figure 3 shows images of the fabricated device, where a 300 nm channel was successfully fabricated. Trypsin was chemically immobilized on the nanochannel surface by crosslinking the APTES molecules and trypsin via glutaraldehyde. Figure 4 shows the results of the immobilized trypsin density obtained from fluorescence immunochemical measurements, and apparent concentration calculated from the density and Eq. (1). The trypsin density obtained by the trypsinogen immobilization process was 2770 molecules/ μm^2 , which represents an apparent trypsin concentration of 15.4 μM . On the other hand, that by the trypsin immobilization process was calculated to be 1100 molecules/ μm^2 , which represents an apparent trypsin concentration of 6.1 μM . Therefore, the trypsinogen immobilization process gave a 2.5 times higher concentration than the trypsin immobilization process. The results suggest that self-digestion during the immobilization process in the nanochannel occurred in the trypsin immobilization process, despite the addition of CaCl_2 at 4 °C to inhibit self-digestion. From these results, it is considered that trypsin introduced in the liquid phase digests immobilized trypsin on the surface during the immobilization process due to the small size of the nanochannel and thus the high surface-to-volume ratio. On the other hand, self-digestion was not induced by the trypsinogen process, in principle. Therefore, the immobilized trypsin density from the trypsinogen process was higher than that from the trypsin process because self-digestion was not induced during the former immobilization process. In addition, compared to the bulk limit concentration (approximately 0.5

1
2
3
4
5
6 μM), the concentration with a picoliter enzyme reactor produced with the trypsinogen
7
8
9 immobilization process was 36 times higher. In a conventional enzyme immobilized reactor using
10
11
12 packed beads or monolith columns, measurements of enzyme density are difficult. Therefore, the
13
14
15 results of this study are useful to achieve an understanding of enzyme immobilization on the
16
17
18 surface of a small space, and the proposed trypsinogen immobilization process in a small space
19
20
21 has been confirmed to improve the enzyme density. In addition, to evaluate nonspecific trypsin
22
23
24 adsorption, the average trypsin density and apparent concentration in the outer side of trypsin
25
26
27 immobilized region in the nanochannel was shown in Figure 4. Due to significant inhibition of
28
29
30 nonspecific adsorption by PEG, nonspecific adsorption of trypsin on the nanochannel was
31
32
33 negligible.

34
35
36 In the enzyme reaction measurements, the reaction time was determined at flow
37
38
39 velocities obtained from the arrival time of the reacted sample at the detection point (Figure S2).
40
41
42 The product concentration was determined by the calibration of POPS signal of a BAPNA sample
43
44
45 100%-digested by 0.01 mg/mL trypsin solution at 25 °C for over 24 h in the bulk, and the POPS
46
47
48 signal of the BAPNA sample was defined as 0% digestion. Figure S3(a) showed POPS signals of
49
50
51 100%-digested BAPNA, 0%-digested BAPNA, and BAPNA after 0.7 min reaction. From the
52
53
54 calibration, the product concentration of BAPNA after 0.7 min reaction was determined to be 64
55
56
57 μM (50% digestion). Figure 5 shows the product concentration and digestion rate as a function of
58
59
60

1
2
3
4
5
6 the reaction time. The reaction time for the picoliter enzyme reactor to reach 95% digestion rate
7
8
9 was 4.6 min, while that of the bulk reaction was 115 min. Therefore, the enzyme reaction in the
10
11
12 picoliter enzyme reactor was accelerated 25 times compared to that in the bulk by the 36 times
13
14
15 higher enzyme concentration (picoliter enzyme reactor: 15.4 μM , bulk reaction: 0.01 mg/mL =
16
17
18 0.43 μM). The results suggest that only 30 min would be required for protein digestion using the
19
20
21 picoliter enzyme reactor, whereas overnight reaction would be required for protein digestion in
22
23
24 the bulk. Protein digestion within 30 min can prevent artificial modification, and thus reduce the
25
26
27 proteomic sample complexity. Finally, for discussion of enzyme stability, catalytic activity of
28
29
30 immobilized trypsin was investigated. In previous reports, the activity of free trypsin in liquid
31
32
33 phase was gradually decreased during a few hours due to self-digestion.^{23–26} On the other hand,
34
35
36 the activity of immobilized trypsin on the surface was kept for hours-days.^{47,48} In this study, faster
37
38
39 enzyme reaction was realized by using the immobilized trypsin stored in borate buffer for 60
40
41
42 hours at 25 °C after immobilization on the nanochannel. As a result, catalytic activity of
43
44
45 immobilized trypsin in this study showed at least in 60 hours. Consequently, an ultra-fast picoliter
46
47
48 enzyme reactor with a volume of 32.4 pL was successfully developed, which will be a powerful
49
50
51 tool not only for protein digestion in single-cell shotgun proteomics, but also for enzyme
52
53
54 microkinetics study in nanospaces.
55
56
57
58
59
60

Conclusion

In conclusion, an ultra-fast picoliter enzyme reactor using nanochannel. A device which channel depth was 300 nm and volume was 32.4 pL was fabricated. The reaction volume is smaller by orders than conventional bulk reaction or micro-reactor. The picoliter enzyme reactor was prepared by immobilizing trypsinogen which was activated to trypsin by enterokinase. This process does not induce self-digestion during surface modification in principle. As a result, immobilized trypsin density by the trypsinogen immobilization process was 2.5 times higher than that by conventional trypsin immobilization process. Furthermore, apparent enzyme concentration was 36 times higher compared to limit concentration in the bulk. Finally, tryptic hydrolysis reaction using picoliter enzyme reactor was performed. The enzyme reaction in the picoliter enzyme reactor was accelerated 25 times compared to that in the bulk. The picoliter reactor is universally applicable for a reactor which can overcome limitation in the bulk. In addition, using the picoliter enzyme reactor, protein with pL volume will be digested without self-digestion and artificial modification, which will greatly contribute not only to protein digestion in single-cell shotgun proteomics, but also to enzyme microkinetics study in nanospaces.

Conflicts of interest

There are no conflicts of interest to declare

Acknowledgments

The authors would like to thank Prof. Masaya Miyazaki from Kyusyu University and Prof. Kiichi Sato from Gunma University for fruitful discussions. Fabrication and observation facilities were provided in part by the Academic Consortium for Nano and Micro Fabrication of four universities (The University of Tokyo, Tokyo Institute of Technology, Keio University and Waseda University, JAPAN) and Advanced Characterization Nanotechnology Platform of the University of Tokyo, supported by "Nanotechnology Platform" of the Ministry of Education, Culture, Sports, Science and Technology (MEXT), Japan. The authors gratefully acknowledge financial support from Core Research for Evolutional Science and Technology (CREST) of the Japan Science and Technology Agency (JST): JPMJCR14G1.

References

- 1 A. K. Björklund, M. Forkel, S. Picelli, V. Konya, J. Theorell, D. Friberg, R. Sandberg and J. Mjösberg, *Nat. Immunol.*, 2016, **17**, 451–460.
- 2 F. Buettner, K. N. Natarajan, F. P. Casale, V. Proserpio, A. Scialdone, F. J. Theis, S. A. Teichmann, J. C. Marioni and O. Stegle, *Nat. Biotechnol.*, 2015, **33**, 155–160.
- 3 D. Grün, A. Lyubimova, L. Kester, K. Wiebrands, O. Basak, N. Sasaki, H. Clevers and A. Van Oudenaarden, *Nature*, 2015, **525**, 251–255.
- 4 B. Mahata, X. Zhang, A. A. Kolodziejczyk, V. Proserpio, L. Haim-Vilmovsky, A. E. Taylor, D. Hebenstreit, F. A. Dingler, V. Moignard, B. Göttgens, W. Arlt, A. N. J. McKenzie and S. A. Teichmann, *Cell Rep.*, 2014, **7**, 1130–1142.
- 5 J. T. Gaublomme, N. Yosef, Y. Lee, R. S. Gertner, L. V. Yang, C. Wu, P. P. Pandolfi, T. Mak, R. Satija, A. K. Shalek, V. K. Kuchroo, H. Park and A. Regev, *Cell*, 2015, **163**, 1400–1412.
- 6 O. Stegle, S. A. Teichmann and J. C. Marioni, *Nat. Rev. Genet.*, 2015, **16**, 133–145.
- 7 A. Schmid, H. Kortmann, P. S. Dittrich and L. M. Blank, *Curr. Opin. Biotechnol.*, 2010, **21**, 12–20.
- 8 L. Armbrecht and P. S. Dittrich, *Anal. Chem.*, 2017, **89**, 2–21.
- 9 D. R. Reyes, D. Iossifidis, P. A. Auroux and A. Manz, *Anal. Chem.*, 2002, **74**, 2623–2636.
- 10 P. A. Auroux, D. Iossifidis, D. R. Reyes and A. Manz, *Anal. Chem.*, 2002, **74**, 2637–2652.
- 11 M. Tokeshi, T. Minagawa, K. Uchiyama, A. Hibara, K. Sato, H. Hisamoto and T. Kitamori, *Anal. Chem.*, 2002, **74**, 1565–1571.
- 12 Y. Tanaka, K. Sato, M. Yamato, T. Okano and T. Kitamori, *J. Chromatogr. A*, 2006,

- 1
2
3
4
5
6 1111, 233–237.
7
8
9 13 K. Sato, A. Egami, T. Odake, M. Tokeshi, M. Aihara and T. Kitamori, *J. Chromatogr. A*,
10 2006, **1111**, 228–232.
11
12
13 14 M. Goto, K. Sato, A. Murakami, M. Tokeshi and T. Kitamori, *Anal. Chem.*, 2005, **77**,
14 2125–2131.
15
16
17 15 A. Hibara, T. Saito, H.-B. Kim, M. Tokeshi, T. Ooi, M. Nakao and T. Kitamori, *Anal.*
18 *Chem.*, 2002, **74**, 6170–6176.
19
20
21 22 K. Mawatari, Y. Kazoe, H. Shimizu, Y. Pihosh and T. Kitamori, *Anal. Chem.*, 2014, **86**,
23 4068–4077.
24
25
26 27 T. Nakao, Y. Kazoe, K. Morikawa, L. Lin, K. Mawatari and T. Kitamori, *Analyst*, 2020,
28 **145**, 2669–2675.
29
30
31 32 K. Shirai, K. Mawatari, R. Ohta, H. Shimizu and T. Kitamori, *Analyst*, 2018, 943–948.
33
34 35 19 T. Nakao, Y. Kazoe, E. Mori, K. Morikawa, T. Fukasawa, A. Yoshizaki and T. Kitamori,
36 *Analyst*, 2019, **144**, 7200–7208.
37
38 20 H. Shimizu, K. Morikawa, Y. Liu, A. Smirnova, K. Mawatari and T. Kitamori, *Analyst*,
39 2016, **141**, 6068–6072.
40
41
42 43 21 Y. Kazoe, Y. Shimizu, Y. Terui, K. Morikawa, K. Mawatari and T. Kitamori,
44 *Proceeding of MicroTAS*, 2018, 989–990.
45
46
47 22 L. Switzar, M. Giera and W. M. A. Niessen, *J. Proteome Res.*, 2013, 12, 1067–1077.
48
49 23 F. F. Nord, M. Bier and L. Terminiello, *Arch. Biochem. Biophys.*, 1956, **65**, 120–131.
50
51 24 T. Sipos and J. R. Merkel, *Biochemistry*, 1971, 10, 1102.
52
53 25 M. M. Vestling, C. M. Murphy and C. Fenselau, *Anal. Chem.*, 1990, **62**, 2391–2394.
54
55 26 E. J. Finehout, J. R. Cantor and K. H. Lee, in *Proteomics*, 2005, vol. 5, pp. 2319–2321.
56
57 27 H. Yamaguchi and M. Miyazaki, *Proteomics*, 2013, 13, 457–466.
58
59
60

- 1
2
3
4
5
6 28 M. Matsumoto, F. Matsuzaki, K. Oshikawa, N. Goshima, M. Mori, Y. Kawamura, K.
7
8 Ogawa, E. Fukuda, H. Nakatsumi, T. Natsume, K. Fukui, K. Horimoto, T. Nagashima,
9
10 R. Funayama, K. Nakayama and K. I. Nakayama, *Nat. Methods*, 2017, **14**, 251–258.
11
12
13 29 J. BONGERS, E. P. HEIMER, T. LAMBROS, Y. E. PAN, R. M. CAMPBELL and A.
14
15 M. FELIX, *Int. J. Pept. Protein Res.*, 1992, **39**, 364–374.
16
17 30 O. V. Krokhin, M. Antonovici, W. Ens, J. A. Wilkins and K. G. Standing, *Anal. Chem.*,
18
19 2006, **78**, 6645–6650.
20
21
22 31 D. Ren, G. D. Pipes, D. Liu, L. Y. Shih, A. C. Nichols, M. J. Treuheit, D. N. Brems and
23
24 P. V. Bondarenko, *Anal. Biochem.*, 2009, **392**, 12–21.
25
26 32 P. Hao, Y. Ren, A. Datta, J. P. Tam and S. K. Sze, *J. Proteome Res.*, 2015, **14**, 1308–
27
28 1314.
29
30
31 33 M. Miyazaki and H. Maeda, *Trends Biotechnol.*, 2006, **24**, 463–470.
32
33 34 L. Qiao, Y. Liu, S. P. Hudson, P. Yang, E. Magner and B. Liu, *Chem. - A Eur. J.*, 2008,
34
35 **14**, 151–157.
36
37 35 Y. Asanomi, H. Yamaguchi, M. Miyazaki and H. Maeda, *Molecules*, 2011, **16**, 6041–
38
39 6059.
40
41
42 36 S. Matosevic, N. Szita and F. Baganz, *J. Chem. Technol. Biotechnol.*, 2011, **86**, 325–
43
44 334.
45
46 37 T. Tsukahara, K. Mawatari, A. Hibara and T. Kitamori, *Anal. Bioanal. Chem.*, 2008,
47
48 **391**, 2745–52.
49
50
51 38 K. Morikawa, K. Matsushita and T. Tsukahara, *Anal. Sci.*, 2017, **33**, 1453–1456.
52
53 39 Y. Kazoe, Y. Pihosh, H. Takahashi, T. Ohyama, H. Sano, K. Morikawa, K. Mawatari
54
55 and T. Kitamori, *Lab Chip*, 2019, **19**, 1686–1694.
56
57
58 40 K. Shirai, K. Mawatari and T. Kitamori, *Small*, 2014, **10**, 1514–22.
59
60

- 1
2
3
4
5
6 41 Y. Xu, C. Wang, Y. Dong, L. Li, K. Jang, K. Mawatari and T. Kitamori, *Anal. Bioanal.*
7
8 *Chem.*, 2012, **402**, 1011–1018.
9
10 42 R. Ohta, K. Mawatari, T. Takeuchi, K. Morikawa and T. Kitamori, *Biomicrofluidics*,
11
12 2019, **13**, 024104(7pp).
13
14 43 M. Ye, S. Hu, R. M. Schoenherr and N. J. Dovichi, *Electrophoresis*, 2004, **25**, 1319–
15
16 1326.
17
18 44 W. Lin and C. D. Skinner, *J. Sep. Sci.*, 2009, **32**, 2642–2652.
19
20 45 H. Shimizu, K. Mawatari and T. Kitamori, *Anal. Chem.*, 2010, **82**, 7479–7484.
21
22 46 R. Lottenberg, U. Christensen, C. M. Jackson and P. L. Coleman, *Methods Enzymol.*,
23
24 1981, **80**, 341–361.
25
26 47 K. Atacan, B. Çakiroğlu and M. Özacar, *Food Chem.*, 2016, **212**, 460–468.
27
28 48 J. Sun, B. Xu, Y. Shi, L. Yang and H. Le Ma, *Adv. Mater. Sci. Eng.*, 2017; 2017:
29
30 1457072
31
32
33
34
35
36
37
38
39
40
41
42
43
44
45
46
47
48
49
50
51
52
53
54
55
56
57
58
59
60

Figure 1.

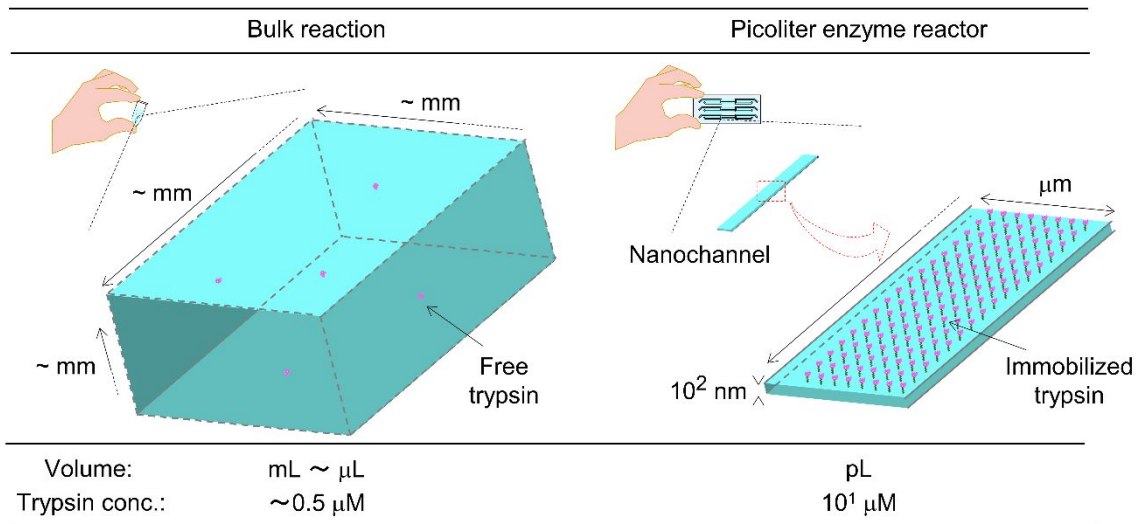


Figure 1. Design and concept of picoliter enzyme reactor. To exceed limit enzyme concentration in bulk, trypsin was immobilized on a nanochannel surface.

Figure 2.

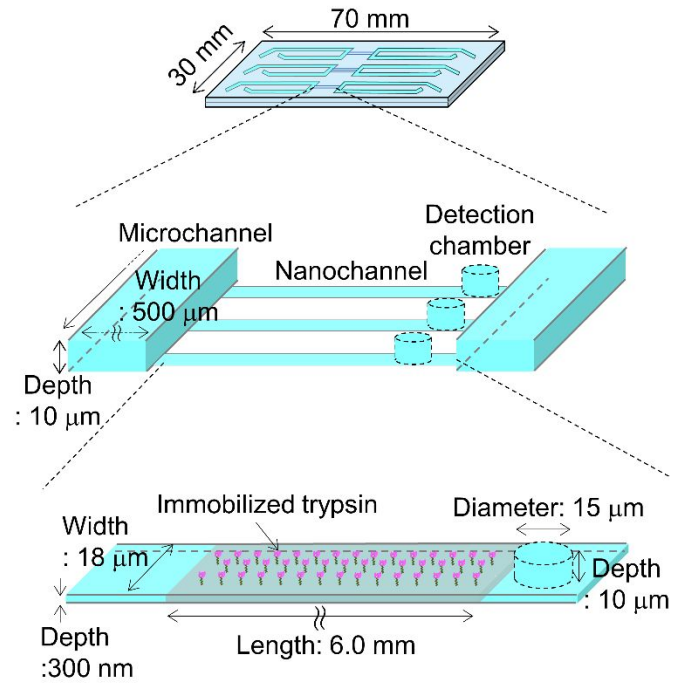


Figure 2. Design of the nanochannel in the picoliter enzyme reactor.

Figure 3.

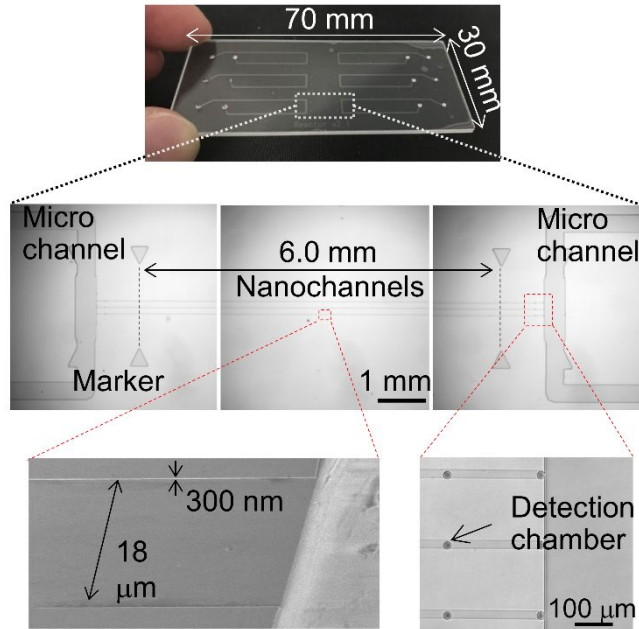


Figure 3. Photo of the device, microscope and SEM images of microchannels and nanochannels.

Figure 4.

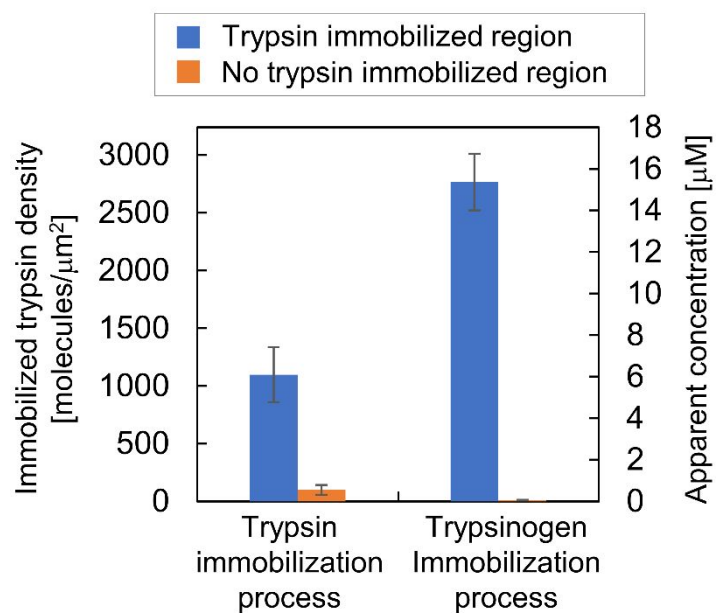


Figure 4. Immobilized trypsin density and apparent concentration of the picoliter enzyme reactor by trypsin immobilization process and trypsinogen immobilization process.

Figure 5.

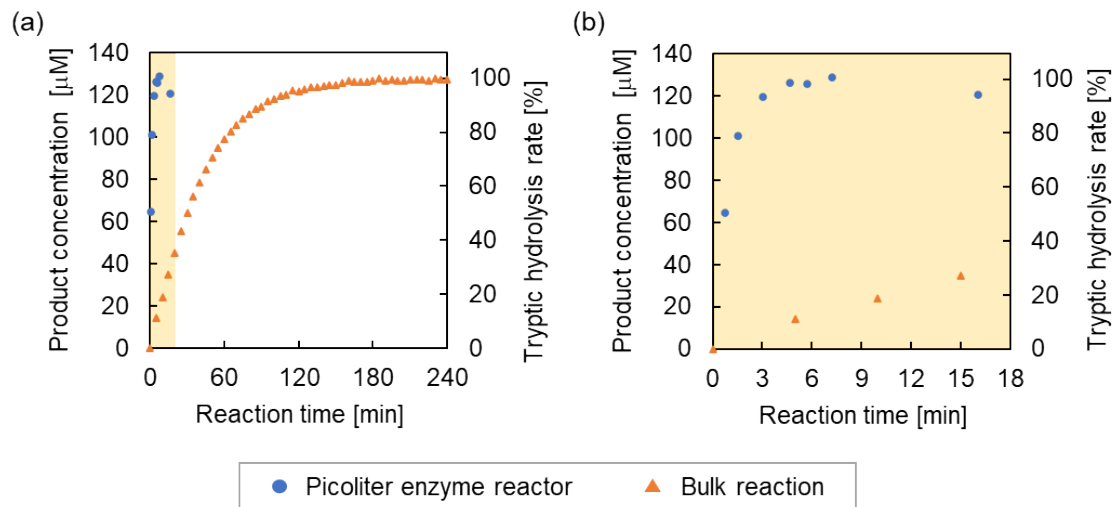
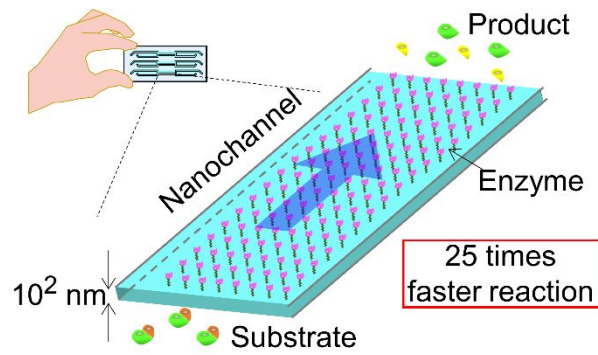


Figure 5. Product concentration and tryptic hydrolysis rate with reaction time in picoliter enzyme reactor and bulk reaction. (b) was magnification of the region of 0-18 min in (a).

1
2
3 Table of contents.
4
5
6
7
8
9
10
11
12
13
14
15
16
17
18
19
20
21
22
23
24
25
26
27
28
29
30
31
32
33
34
35
36
37
38
39
40
41
42
43
44
45
46
47
48
49
50
51
52
53
54
55
56
57
58
59
60



Picoliter enzyme reactor using trypsin immobilized nanochannel realized
25 times faster reaction compared to bulk reaction.